The Cryosphere, 18, 1125–1138, 2024
https://doi.org/10.5194/tc-18-1125-2024

The Cryosphere Open Access EGU

The staggered retreat of grounded ice in the Ross Sea, Antarctica, since the Last Glacial Maximum (LGM)

Matthew A. Danielson and Philip J. Bart

Department of Geology and Geophysics, Louisiana State University, Howe-Russell Geoscience Complex E235, Baton Rouge, LA 70803, USA

Correspondence: Matthew A. Danielson (mdani38@lsu.edu)

Received: 26 June 2023 – Discussion started: 28 July 2023
Revised: 11 January 2024 – Accepted: 24 January 2024 – Published: 8 March 2024

Abstract. The retreat of the West Antarctic Ice Sheet (WAIS) in the Ross Sea after the Last Glacial Maximum (LGM) was more significant than for any other Antarctic sector. Here we combined the available chronology of retreat with new mapping of seismically resolvable grounding zone wedges (GZWs). Mapping GZWs is important because they record the locations of former stillstands in the extent of grounded ice for individual ice streams during the overall retreat. Our analysis shows that the longest stillstands occurred early in the deglacial period and had millennial durations. Stillstands ended abruptly with retreat distances measured in the tens to hundreds of kilometers creating deep embayments in the extent of grounded ice across the Ross Sea. The location of embayments shifted through time. The available chronological data show that cessation of WAIS and East Antarctic Ice Sheet (EAIS) stillstands was highly asynchronous across at least 5000 years. There was a general shift to shorter stillstands throughout the deglacial period. The asynchronous collapse of individual catchments during the deglacial period suggests that the Ross Sea sector would have contributed to multiple episodes of relatively small-amplitude sea-level rise as the WAIS and EAIS retreated from the region. The high sinuosity of the modern grounding zone in the Ross Sea suggests that this style of retreat persists.

1 Introduction

By the peak of the Last Glacial Maximum (LGM), grounded ice had advanced to the outermost continental shelf in the western Ross Sea, Antarctica, and to the continental shelf edge in the eastern Ross Sea (Anderson et al., 2014). The extent of grounded and floating ice was nearly as expansive as it could have been. Six fast-flowing ice streams deeply eroded broad, the foredeepened troughs across the continental shelf. Eroded sediment was transported in basal ice and/or subglacially (Alley et al., 2007, 1989; Powell et al., 1996; Prothro et al., 2018; Christoffersen et al., 2010). The sediment was ultimately deposited either on the outer continental shelf or upper-slope depocenters (Shipp et al., 1999). In the western Ross Sea, foredeepened Drygalski Trough (DT), JOIDES Basin (JB), and Pennell Trough (PT) extend to the continental shelf edge and were eroded during several successive glacial maxima. The outer parts of these troughs were partly backfilled with large-scale grounding zone wedges (GZWs) during and/or after the LGM. In the eastern Ross Sea troughs, where ice had reached the continental shelf edge, large trough-mouth fans were deposited on the upper slope (Mosola and Anderson, 2006). During the post-LGM retreat, grounding line retreat paused within the outer reaches of the Glomar Challenger Basin (GCB), Whales Deep Basin (WDB), and Little America Basin (LAB) for a sufficiently long time to deposit large GZWs (i.e., several tens of meters thick and tens of kilometers long) (Mosola and Anderson, 2006; Bart and Owolana, 2012). The GZW sediment volumes partly reflect durations of grounding line stillstands for individual ice streams (Bart and Cone, 2012; Bart et al., 2017; Bart and Owolana, 2012). Several previous studies have focused on the changing extent of grounded and floating ice and the timing of post-LGM retreat (Conway et al., 1999; Domack et al., 1999; Mosola and Anderson, 2006). Anderson et al. (2014) conducted the last Ross Sea synthesis of seismic stratigraphy and radiocarbon dates. More recently, Halberstadt et al. (2016) conducted a detailed eval-

uation of legacy multibeam data and identified GZWs and mega-scale glacial lineations associated with the LGM and post-LGM GZW stillstands. These stratigraphic data provide abundant evidence as to the progression of West Antarctic Ice Sheet (WAIS) and East Antarctic Ice Sheet (EAIS) retreat based on stratigraphic superposition. Here we build on the Halberstadt et al. (2016) study of seafloor morphology by mapping the sediment volume of the GZWs across the six basins of the Ross Sea to evaluate the duration of individual grounding zone stillstands. Establishing the former durations of GZWs is important to understand the regional-scale ice sheet retreat in the Ross Sea and thus how ice-volume changes from Antarctica contributed to global sea level in the past. The paleo-perspective also informs our understanding of how additional contraction might proceed and contribute to future sea-level rise.

2 Methods

2.1 Regional seismic grid

Our study generated regional stratigraphic correlations of bounding surfaces across 22 surveys of multi- and single-channel reflection seismic data acquired from across the Ross Sea (Table S1 in the Supplement). The surveys include 510 seismic lines with a total coverage of $\sim 54\,000$ km. The data are currently stored and maintained at the Antarctic seismic data library system (SDLS) at the Italian National Institute of Oceanography and Applied Geophysics (OGS) and have been used in previous studies such as Perez et al. (2021). Our mapping focused on GZWs interpreted to be of LGM and post-LGM ages, complementing the analyses of seafloor morphology by Halberstadt et al. (2016). The seismic profiles were interpreted in Petrel (Fig. 1). The digital data used in this study have been processed prior to being archived at the SDLS. Individual seismic lines were imported as SEG-Y files into the software using separate files containing navigation data.

2.2 Seismic interpretation and isopach mapping of LGM and post-LGM GZWs

We focused on the seismically resolvable LGM and post-LGM GZWs throughout the Ross Sea that have been identified in previous seismic studies (Shipp et al., 1999; Mosola and Anderson, 2006; Bart and Owolana, 2012; Bart and De Santis, 2012; Bart et al., 2017). This includes GZWs identified in legacy multibeam data (Halberstadt et al., 2016). The seafloor reflection and the unconformities bounding the top and base of the GZWs in each trough on the deglaciated Ross Sea shelf were mapped using regional seismic stratigraphy and comparison to previous studies. Additional single-channel paper seismic lines from four surveys (NBP9307, NBP9401, NBP9501, and NBP9902) were used to supplement the interpretation of major GZW features. These interpretations were completed on paper and then imported into Petrel using navigation files as a set of points in two-way travel time (TWTT).

Two-way-travel time maps were made using convergent interpolation in Petrel with a cell size of 50 m, where the computer-interpreted horizons were the primary input and the paper-interpreted data were secondary input. Time-structure maps were made by subtracting the map of the GZW base from the seafloor map. Refraction sonobuoy measurements in the Ross Sea provide a regional record of sediment velocities (Cochrane et al., 1995, 1992). The points of the sonobuoy measurements taken from four expeditions were plotted in Petrel and interpolated to create depth and interval velocity maps. All the analyzed GZW deposits were in shallow layers of sediment (upper 250 ms), and thus only the uppermost interval velocity map was used. This section has velocities that vary from 1700 to 2200 $\mathrm{m\,s^{-1}}$ across the region (Fig. S1 in the Supplement). The interval velocity map was then used as an input to build a velocity model in Petrel. Time-structure maps were then depth-converted using the velocity model to create isopach maps for each GZW.

2.3 Volume and duration calculation

The isopach maps were used to calculate sediment volumes for the GZWs in QGIS software. The sediment volumes were then used as a basic parameter to estimate stillstand duration. The paleo-sediment flux for each of the paleo-ice streams in the Ross Sea (Eq. 1) is defined as Q_s. The paleo-sediment flux of an ice stream is the product of the paleo-drainage area (A) and average sediment yield (S) at the grounding zone where sediment is sourced from upstream subglacial erosion. Our estimates use a simple assumption of the sediment yield and paleo-drainage area. The sediment yield of $0.7 \pm 0.21\ \mathrm{mm\,yr^{-1}}$ derived by Bart and Tulaczyk (2020) for the WDB drainage area was applied to the adjacent catchment of the LAB to infer a paleo-flux. The $0.7 \pm 0.21\ \mathrm{mm\,yr^{-1}}$ sediment yield was derived for the WDB middle shelf GZW which was determined to have been deposited during a stillstand whose onset and cessation dates are constrained by radiocarbon dates (Bart et al., 2018). For the western Ross Sea troughs of the PT, JB, and DT, we used a sediment yield of $0.49 \pm 0.21\ \mathrm{mm\,yr^{-1}}$, which is a value 30 % less than the WDB value. This is due to the presence of crystalline and lithified sedimentary bedrock in the western Ross Sea (Greenwood et al., 2021). A 30 % lower sediment yield would be expected for a catchment floored by crystalline bedrock due to a higher resistance to erosion (Schlunegger et al., 2001). The GCB received flow from both East and West Antarctica during the LGM (Licht et al., 2005). Thus, the sediment yield of $0.7 \pm 0.21\ \mathrm{mm\,yr^{-1}}$was used for the parts of the drainage area from West Antarctica (Kamb, Whillans, Mercer ice streams) and the eastern Ross Sea shelf, while the sediment yield of $0.49 \pm 0.21\ \mathrm{mm\,yr^{-1}}$was used for the contribution

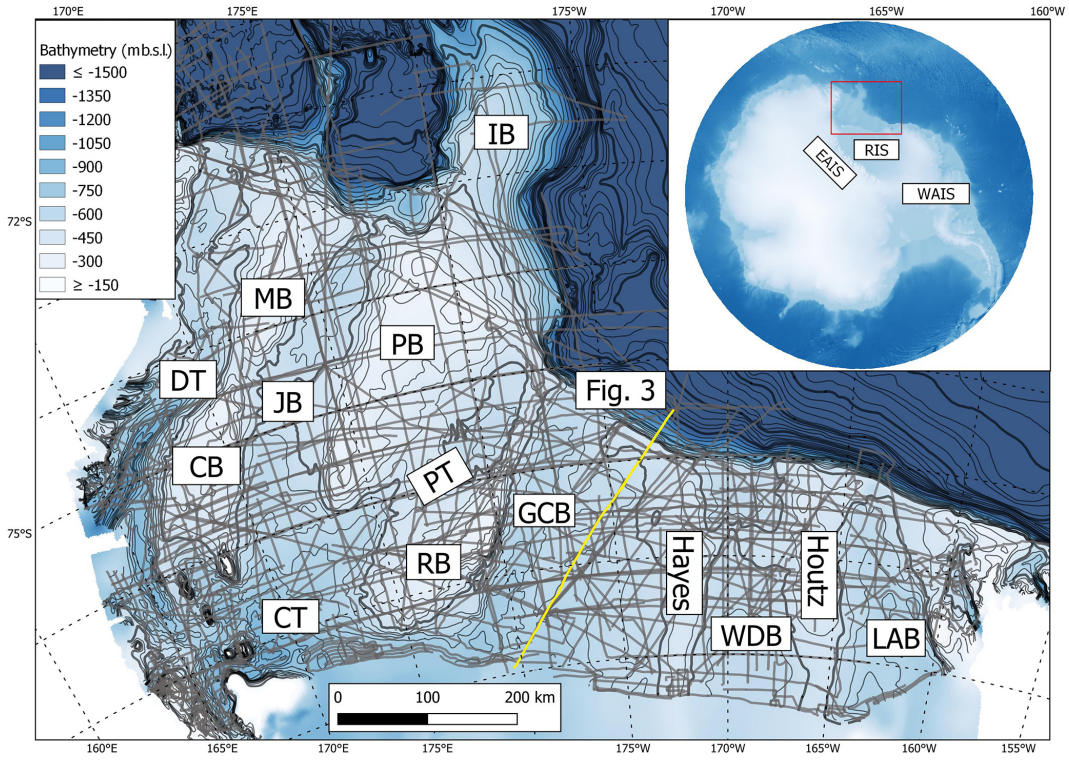

Figure 1. Map of the Ross Sea showing seismic coverage. Bathymetry is from Davey and Nitsche (2013). Inset map of Antarctica using the International Bathymetric Chart of the Southern Ocean ice surface and bathymetry grid showing the locations of the East Antarctic Ice Sheet (EAIS) and the West Antarctic Ice Sheet (WAIS) in addition to the position of the Ross Ice Shelf (RIS) (Dorschel et al., 2022). Main map shows Ross Sea as indicated by the red box on the inset map. Labels of bathymetric troughs on the Ross Sea shelf are as follows: LAB – Little America Basin; WDB – Whales Deep Basin; GCB – Glomar Challenger Basin; PT – Pennell Trough; CT – Central Trough; JB – JOIDES Basin; DT – Drygalski Trough. Labels of bathymetric banks on the Ross Sea shelf are as follows: Houtz – Houtz Bank; Hayes – Hayes Bank; RB – Ross Bank; PB – Pennell Bank; IB – Iselin Bank; MB – Mawson Bank; CB – Crary Bank. The position of the Fig. 3 seismic profile is indicated with the yellow line.

from the outlet glaciers in East Antarctica, such as Beardmore Glacier (Fig. 2).

$$Q_s = AS \tag{1}$$

Paleo-drainage areas were estimated for each of the paleo-troughs of the Ross Sea using the drainage area of the present-day WAIS ice streams and EAIS outlet glaciers and projecting their extents into each of the troughs on the outer continental shelf (Fig. 2). The terminus of each paleo-drainage area is the seaward edge of its respective grounding zone wedge. The approach assumes single-ice-stream capture for the WDB and LAB. The GCB received drainage from the combination of the Kamb, Whillans, and Mercer ice streams based on the sub-ice-shelf topography shown in the ROSETTA project in addition to other East Antarctic glaciers (Tinto et al., 2019; Licht et al., 2005). The JB and PT shared capture from Byrd and other smaller East Antarctic catchments. The upstream drainage area shared by the JB and PT was halved for calculations to reflect the shared source of sediment. The DT primarily received ice flow from David Glacier during the LGM (Licht and Palmer, 2013; Licht et al., 2014). There was a reorganization in flow in the southern region of the western Ross Sea during the retreat that is marked by backstepping geomorphological evidence towards David Glacier (Greenwood et al., 2018). Thus, the paleo-flux for the GZW mapped within the interior middle shelf of the JB nearest to Franklin Island (Fig. 4m; Table 1) was calculated using a modified drainage area from the Mawson, Mackay, and David glaciers with no input from Byrd Glacier (Fig. 2). Grounding duration at each location was calculated using the method following Bart and Tulaczyk (2020), where ΔT is the grounding duration, V is the total volume of GZW sediment, and Q_s is the paleo-sediment flux (Eq. 2).

$$\Delta T = \frac{V}{Q_s} \tag{2}$$

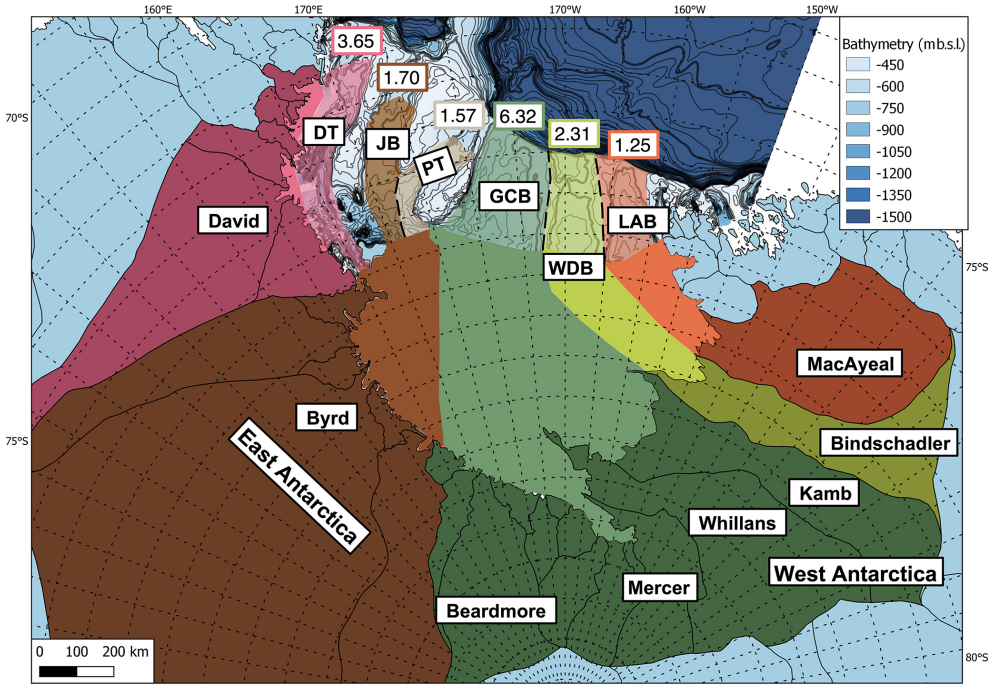

Figure 2. Estimated paleo-drainage catchments for each of the major troughs across the Ross Sea during the LGM. The darker shades correspond to the present-day drainage areas, while the lighter shades correspond to the projected paleo-drainage into the troughs when the ice sheet extent was expanded. Orange – LAB; yellow – WDB; green – GCB; brown – Pennell and JOIDES; pink – Drygalski Trough. The heavy dashed black line shows the separation between paleo-drainage of adjacent troughs. Drygalski Trough, JOIDES Basin, and Pennell Trough capture drainage from East Antarctic glaciers. The upstream drainage area for JOIDES Basin and Pennell Trough is shared with the area upstream of the dashed black flow divide being divided by 2 for the calculations. The GCB drained a combination of WAIS paleo-ice streams and EAIS outlet glacier flow. The LAB and WDB received sediment from individual WAIS paleo-ice streams. LGM paleo-drainage areas are labeled for each trough, where each label is shown in the form of 10^5 km^2. Modern drainage area polygons are defined by IMBIE 2016 (Mouginot et al., 2017; Rignot et al., 2013).

Table 1. Summary table of GZWs shown in Fig. 4 with drainage area, volume, paleo-sediment flux, and duration with respective uncertainties.

GZW location	Estimated paleo-drainage area, A (10^5 km^2)	GZW volume, V (km^3)	Paleo-sediment flux, Q (10^8 m^3 a^{-1})	Duration, ΔT (years)
a. LAB outer shelf	1.25	301 ± 19	0.87 ± 0.26	3445 ± 1136
b. LAB middle shelf	1.11	120 ± 8	0.79 ± 0.23	1535 ± 506
c. LAB middle shelf inner reaches	1.05	33 ± 3	0.74 ± 0.22	453 ± 149
d. WDB outer shelf	2.31	216 ± 16	1.62 ± 0.49	1027 ± 419
e. WDB middle shelf	2.23	534 ± 35	1.67 ± 0.47	3200 ± 700
f. GCB outer shelf	6.32	610 ± 41	4.10 ± 1.33	1487 ± 455
g. GCB middle shelf west	6.17	523 ± 33	4.00 ± 1.30	1308 ± 399
h. GCB inner reaches east	5.80	47 ± 7	3.74 ± 1.22	126 ± 38
i. GCB inner reaches west	5.93	33 ± 4	3.83 ± 1.24	87 ± 27
j. GCB inner reaches Ross Bank	5.72	45 ± 4	3.68 ± 1.20	121 ± 37
k. PT middle shelf	1.57	69 ± 8	0.77 ± 0.33	898 ± 207
l. JOIDES middle shelf	1.70	421 ± 37	0.83 ± 0.36	5072 ± 1170
m. JOIDES inner reaches 1	0.90	58 ± 6	0.44 ± 0.19	1340 ± 309
n. JOIDES inner reaches 2	1.48	117 ± 11	0.73 ± 0.31	1612 ± 372
o. DT outer shelf	3.65	583 ± 21	1.79 ± 0.77	3257 ± 752
p. DT inner reaches 1	1.17	48 ± 5	0.57 ± 0.25	844 ± 195
q. DT inner reaches 2	1.17	20 ± 1	0.57 ± 0.25	350 ± 81

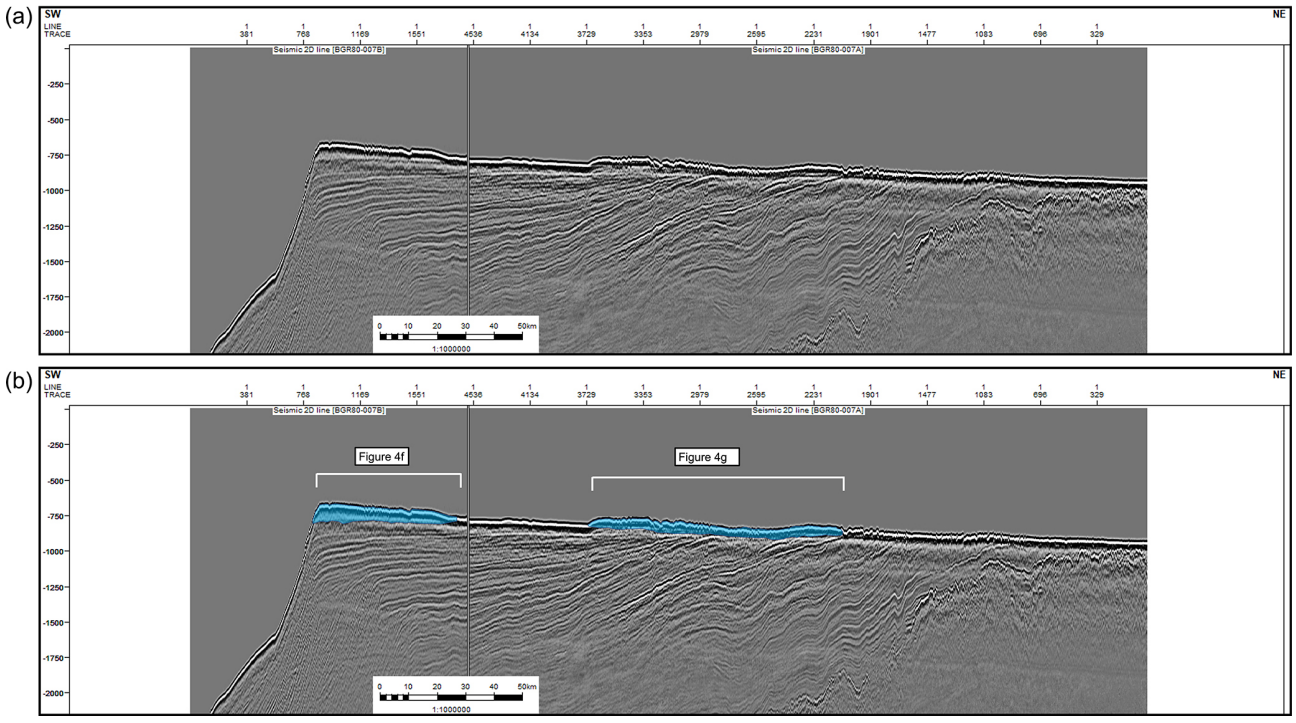

Figure 3. Uninterpreted **(a)** and interpreted **(b)** seismic line BGR80-007 through the GCB. Location of line is indicated with Fig. 1. Blue shaded region shows interpreted GZWs. Position of GZWs and thickness map are shown in Fig. 4.

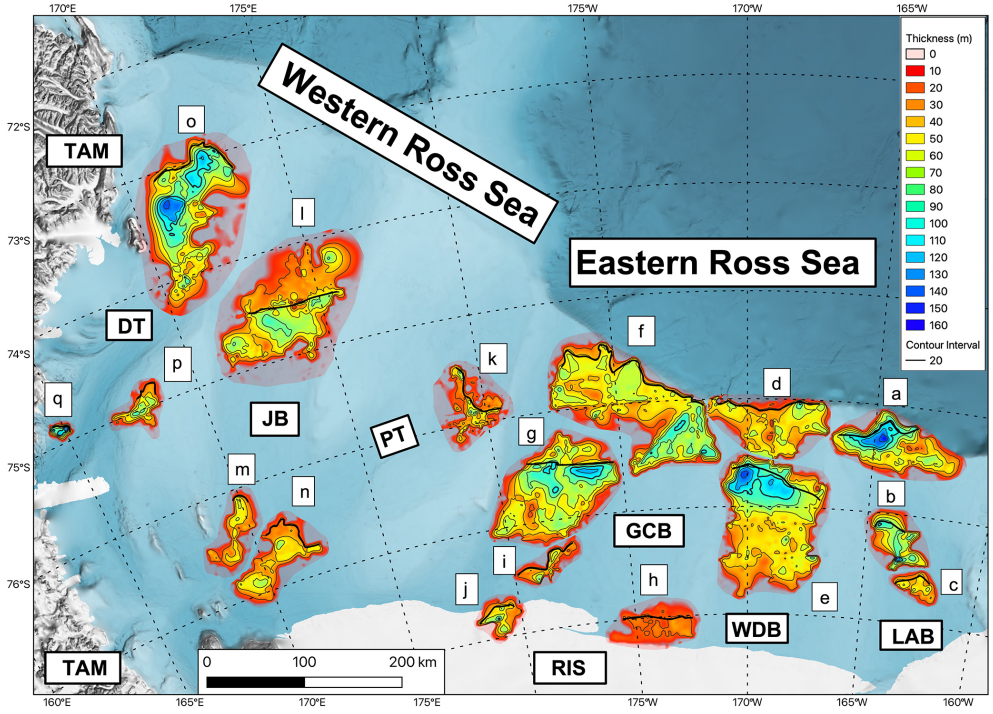

Figure 4. Thicknesses contour maps of Ross Sea GZWs. The heavy black line shows the approximate location of boundary between the GZW topset and foreset. GZWs are labeled "a" to "q" starting in the east with the LAB outer shelf GZW. Letter labels of GZWs correspond to records in Table 1. Contour interval: 20 m. Labels of geometric features are as follows: LAB – Little America Basin; WDB – Whales Deep Basin; GCB – Glomar Challenger Basin; PT – Pennell Trough; CT – Central Trough; JB – JOIDES Basin; DT – Drygalski Trough; TAM – Transantarctic Mountains; RIS – Ross Ice Shelf. Bathymetry shown in the base map is from IBSCO v2 (Dorschel et al., 2022).

Table 2. Drainage areas and paleo-flux of LGM positions with respective uncertainties.

	Little America	Whales Deep	Glomar Challenger	Pennell	JOIDES	Drygalski
Drainage area (10^5 km^2)	1.25	2.31	6.32	1.57	1.70	3.65
LGM paleo-sediment flux (10^8 m^3 a^{-1})	0.87 ± 0.26	1.62 ± 0.49	4.10 ± 1.33	0.77 ± 0.33	0.83 ± 0.36	1.79 ± 0.77

3 Results

3.1 Seismically resolvable GZWs on the Ross Sea shelf

Stratigraphic correlations on the regional seismic transects yielded two-way travel time maps for the Ross Sea outer continental shelf and middle continental shelf (Fig. S2). The inner continental shelf is covered by the Ross Ice Shelf and hence cannot be investigated using the marine seismic profiles used in this study. Mapped horizons bound GZWs from the base of the LGM unconformity to the seafloor (Fig. 3). Seventeen GZWs were identified and mapped within the Ross Sea trough basins (Appendix A; Table S3). Fourteen of these GZWs (Fig. 4a–h, k–m, o–q; Table 1) have been identified from previous studies (e.g., Anderson et al., 2014; Halberstadt et al., 2016). Three new GZWs were mapped from the regional seismic data in the inner reaches of the middle continental shelf sectors of the JB, PT, and GCB (Fig. 4i–j, and n; Table 1). The WDB and PT have two GZWs at the shelf edge and on the middle continental shelf. The JB has a GZW at the middle continental shelf and two proximal to the modern ice shelf calving front in the inner reaches of the trough. The GCB, which has the largest drainage area of all the paleo-ice streams, has five GZWs with one at the shelf edge, one on the middle shelf, and three in the inner reaches of the trough proximal to the modern ice shelf calving front (Table 2; Fig. 4).

In the eastern Ross Sea, the shelf edge and outer continental shelf GZWs define part of the modern banks. In the western Ross Sea, the GZWs are trough-confined except for the inner reaches of the middle continental shelf GZWs in the DB that were deposited on the banks adjacent to the foredeepened section of the trough (Baroni et al., 2022). Time-structure maps were generated for the top and base of each GZW and depth-converted. The difference between these two surfaces gives thickness maps for the 17 GZWs in the Ross Sea (Fig. 4).

3.2 Grounding durations of Ross Sea GZWs

Sediment volumes for each GZW are shown in Table 1. The outer shelf GZWs in the WDB, GCB, JB, and DT are the largest with sediment volumes on the order of 10^3 km^3. The inner reaches of the middle continental shelf GZWs have the smallest volumes on the order of 10^2 km^3. The drainage area for the ice streams that deposited these GZWs includes the projected paleo-ice stream drainage pathways (Fig. 2) up to the topset–foreset boundary of the mapped GZW. Paleo-flux values are estimated from the product of drainage area with the sediment yield. Stillstand duration was then calculated from the paleo-sediment fluxes and GZW sediment volumes (Tables 2 and 3).

The JB outer continental shelf GZW has the longest duration of ~ 5.0 kyr. The inner reaches of the middle continental shelf GZWs in the GCB have the shortest durations on the order of 10^1–10^2 years. Duration calculations include an uncertainty of ± 2 ms from uncertainty in the TWTT measurement of the GZWs as well as a ± 50 m s^{-1} uncertainty from the velocity model used to convert the TWTT maps to depth.

4 Discussion

4.1 Stillstand durations on the Ross Sea continental shelf

4.1.1 Millennial-scale stillstand durations on the outer and middle continental shelf

We present durations estimated using the sediment yield from the WDB middle continental shelf stillstand for the eastern Ross Sea troughs and a yield that is 30 % less for the western Ross Sea troughs. The durations for the GCB were calculated using both yields to reflect the drainage from both East and West Antarctica. The calculated durations suggest that the largest GZWs in the Ross Sea had stillstands lasting up to a few millennia (Table 4). This general assessment is strongly supported by radiocarbon dates using benthic foraminifera collected in the till of the WDB middle continental shelf stillstand (Bart et al., 2018). The dates suggest that the stillstand had begun by 14.7 ± 0.4 cal kyr BP before retreating by 11.5 ± 0.3 cal kyr BP. The GZWs on the Ross Sea shelf are generally larger than those on other Antarctic continental shelves (Batchelor and Dowdeswell, 2015). In the eastern Ross Sea troughs, larger sediment volumes are partly related to ice stream erosion across the broad West Antarctic catchment areas much of which is underlain by sedimentary bedrock (Tinto et al., 2019). In the western Ross Sea troughs, there was expanded flow from East Antarctic glaciers through the Transantarctic Mountains during the LGM that provided sediment flux (Licht et al., 2005; Licht and Palmer, 2013). Exposed outcrops in the Transantarctic Mountains suggest that the bedrock that underlaid the expanded flow was primarily crystalline bedrock and metasediments (Li et al., 2020). The high sediment flux and widespread sediment aggradation at the grounding lines

Table 3. GZW volumes (km^3) arranged by Ross Sea shelf position with uncertainty.

Shelf position		Little America	Whales Deep	Glomar Challenger	Pennell	JOIDES	Drygalski
1.	Outer continental shelf	301 ± 19	216 ± 16	610 ± 41			583 ± 21
2.	Middle continental shelf	120 ± 8	534 ± 35	523 ± 33	69 ± 8	421 ± 37	
3.	Inner middle continental shelf	33 ± 3		47 ± 7, 45 ± 4, 33 ± 4		58 ± 6, 117 ± 11	48 ± 5, 20 ± 1

Table 4. GZW durations arranged by Ross Sea shelf position with uncertainty. All durations are presented in years.

Shelf position		Little America	Whales Deep	Glomar Challenger	Pennell	JOIDES	Drygalski
1.	Outer continental shelf	3445 ± 1136	1027 ± 419	1487 ± 455			3257 ± 752
2.	Middle continental shelf	1535 ± 506	3200 ± 700	1308 ± 399	898 ± 207	5072 ± 1170	
3.	Inner middle continental shelf	453 ± 149		126 ± 38, 121 ± 37, 87 ± 27		1340 ± 309, 1612 ± 372	844 ± 195, 350 ± 81

(Table 3) would have also contributed to long stillstands by countering the effect of ice stream thinning associated with the deglaciation as flow accelerates, sea level rises, and global climates warm (Anandakrishnan et al., 2007).

4.1.2 Variable stillstand durations between troughs

Our data suggest that the grounding line stillstands on the Ross Sea shelf were of millennial and centennial durations. We focus on comparisons to the WDB middle continental shelf stillstand because its duration is constrained by radiocarbon dates (Bart et al., 2018). In map view, the WDB middle continental shelf appears to be in regional alignment to the outer continental shelf GZWs in the DT and JB and the middle continental shelf GZWs in the PT, GCB, and LAB (Fig. 4). Comparison between the middle continental shelf stillstand durations shows that the PT, LAB, and GCB stillstand durations are shorter than the WDB stillstand duration. The lower durations for the GCB are a result of a higher paleo-drainage area despite the similar volumes. The outer continental shelf stillstand in the DT has a comparable duration to the WDB stillstand. The middle continental shelf stillstand for the JB has the longest duration of ~ 5 kyr.

4.1.3 Stillstand durations within individual troughs

By stratigraphic superposition, GZWs on the outer continental shelf are older than those on the middle continental shelf. Within those basins with more than one GZW, e.g., the LAB, our data suggest significant reductions in stillstand durations as the deglacial period progressed. The shift to shorter stillstands on the inner reaches of the middle continental shelf is generally consistent with tenets of the marine-ice-sheet-instability hypothesis, which predicts unstable grounding line retreat across the foredeepened continental shelf (Weertman, 1974; Joughin and Alley, 2011). After the deposition of a GZW in the interior of the JB and PT (Fig. 4n; Table 1), there was a reorganization in the flow to primary input from Mawson and Mackay glaciers (Greenwood et al., 2018). Thus, the smaller volume GZW deposited near Franklin Island (Fig. 4m; Table 1) has a similar duration to the previous stillstand position. Grounding zone deposits that are too small or thin to map with seismic data are reported from several of the Ross Sea shelf troughs from high-resolution swath bathymetry (Halberstadt et al., 2016; Simkins et al., 2017; Greenwood et al., 2018; Bart and Kratochvil, 2022). We follow other studies that suggest these small-scale features would logically correspond to decadal and/or annual time frames (Livingstone et al., 2016; Dowdeswell et al., 2019).

4.2 Post-LGM erosion rates in the Ross Sea

A key assumption of our study is that erosion rates ranged from 0.7 ± 0.21 to $0.49 \pm 0.21\,mm\,yr^{-1}$ for West and East Antarctic catchments, respectively. This relatively broad range overlaps with the erosion rate estimates for a modern WAIS ice stream (Alley et al., 1986, 1987). The yields are also within the range of erosion for land-based glaciers from Norway, Svalbard, and Switzerland and upper-slope Bear Island trough-mouth fan depocenters (Elverhøi et al., 1998). These and other studies show that yield is affected by the degree of ice cover, regional climate and associated precipitation, and presence or absence of meltwater. All the Ross Sea catchments are south of 70° S, and over the post-LGM time frames we considered, the climates were uniformly colder

Table 5. Grounding start date model for the middle continental shelf GZWs.

GZW location	Retreat mode duration, ΔT (years)	Nearest retreat date (cal yr BP)	Grounding start date (cal yr BP)	Date reference
b. LAB middle shelf	1535	$8715^{b} \pm 70$	$10\,250 \pm 70$	NBP0802 PC2 7–9 cm (Bart and Cone, 2012)
e. WDB middle shelf	3200	$11\,500^{b} \pm 300$	$14\,701 \pm 300$	NBP1502B KC07 (Bart et al., 2018)
g. GCB middle shelf west	1308	$8715^{b} \pm 50$	$10\,023 \pm 50$	NBP0802 PC2 7–9 cm (Bart and Cone, 2012)
k. PT middle shelf	898	$15\,121^{b} \pm 270$	$16\,019 \pm 270$	NBP1502A KC17 144–145 cm (Prothro et al., 2020)
l. JOIDES middle shelf	5072	$13\,315^{a} \pm 240$	$18\,387 \pm 240$	NBP1502A KC48 (Prothro et al., 2020)
o. DT outer shelf	3257	$16\,519^{b} \pm 260$	$19\,776 \pm 260$	NBP9501 KC37 (Prothro et al., 2020; Anderson et al., 2014; Cunningham et al., 1999)

[a] Acid-insoluble inorganics bulk sediment date. [b] Benthic carbonate material from grounding zone sedimentation.

than present (Cuffey et al., 2016). The catchments were all entirely covered by grounded ice so the degree of glaciation could not have been a significant contributor to erosion rate differences between drainage areas. There is no evidence of warmer-than-present intervals that might have significantly increased meltwater production that would have contributed to high end erosion rates (Cuffey et al., 2016). The lowest erosion rates are expected for large catchments with slow-flowing cold ice (Hallet et al., 1996). Deglacial erosion rates are expected to be high because of the rapid flow of warmer ice (Kingslake et al., 2018; Koppes and Montgomery, 2009).

Additional controls on erosion rates and stillstand durations are subglacial topography, subglacial geology, and external atmospheric or oceanographic forcing. Topographic controls on ice stream flow include bottleneck effects from a cross-sectional constriction of the trough as well as localized highs of the seafloor (Dowdeswell and Fugelli, 2012; Mckenzie et al., 2023; Danielson and Bart, 2019). Variations in subglacial geology can also impact erosion rates and stillstand durations where less erodible crystalline and indurated sedimentary bedrock can facilitate longer-duration grounding zone deposition (Klages et al., 2015). Bedrock outcropping at the seafloor can decelerate ice sheet retreat and trigger stillstands (Klages et al., 2014). For the GZWs mapped in this study, there was no presence of outcropping bedrock. External climatic forcing is an important control on grounding line stability. Model results suggest that different ocean and atmosphere forcing combinations in the early deglacial are important for controlling the timing and pattern of retreat (Lowry et al., 2020). Changes in the subglacial topography, substrate type, or external climatic forcing could have contributed to variations in erosion rates across the Ross Sea troughs, and this is reflected in our uncertainty estimates.

All the West Antarctic catchment area is underlain by unconsolidated sediments and sedimentary strata save for small areas of exposed basement (Wilson and Luyendyk, 2006; Jordan et al., 2020; Anderson and Bartek, 1992). Substrates are expected to have similar erodibilities. Thus, the sediment yield of $0.7 \pm 0.21\,\mathrm{mm\,yr^{-1}}$ derived by Bart and Tulaczyk (2020) for the WDB drainage area is most appropriate for the eastern Ross Sea troughs of the LAB and WDB. The East Antarctic parts of the Ross Sea catchments are underlain by less erodible crystalline rocks and lithified sedimentary bedrock (Greenwood et al., 2021). Yields from basement rock are lower by 30 % compared to sedimentary strata (Schlunegger et al., 2001). The sediment yield of $0.49 \pm 0.21\,\mathrm{mm\,yr^{-1}}$ is then most appropriate for the western Ross Sea troughs of the PT, JB, and DT, where a less erodible substrate would produce lower average sediment fluxes.

4.3 A staggered post-LGM retreat of grounding lines in the Ross Sea

Grounding line retreat from the DT outer continental shelf stillstand is estimated to have occurred at 16.5 cal kyr BP (Prothro et al., 2020; Anderson et al., 2014; Cunningham et al., 1999). Prothro et al. (2020) used benthic foraminifera from glacial proximal sediments to show that middle shelf grounding zone stillstands in the JB and PT ended at 15.1 and 13.3 cal kyr BP, respectively. Radiocarbon dates from the WDB show that ice had retreated from the shelf edge by 14.7 ± 0.3 cal kyr BP and that retreat from the middle con-

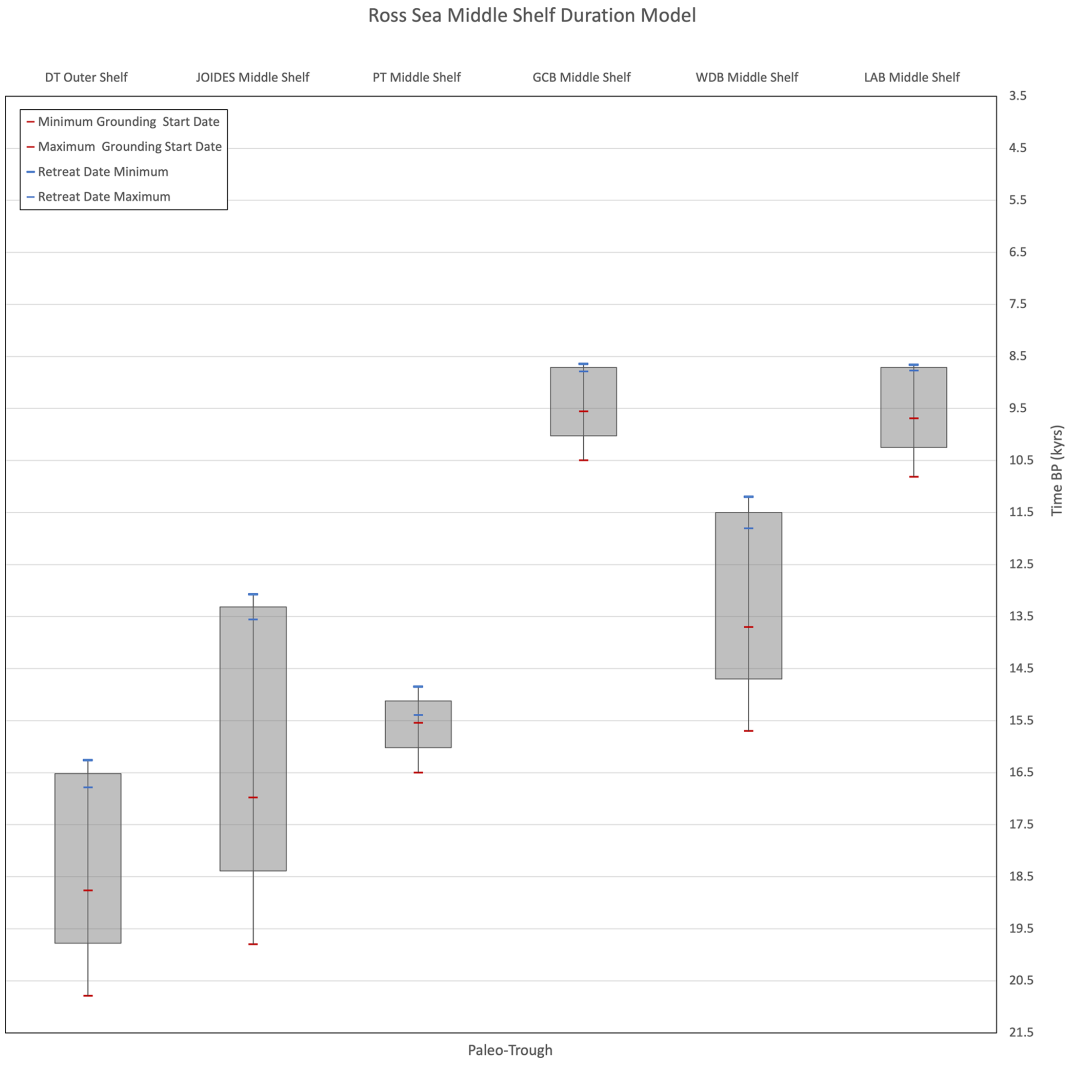

Figure 5. Duration age model for the middle continental shelf GZWs in the Ross Sea using the durations and nearest retreat date plotted in Table 5. The gray box shows the median grounding zone retreat date added to the estimated duration to yield a grounding start date. Blue markers show the uncertainty of the retreat date. Red markers show the uncertainty of the retreat date added to the duration yielding minimum and maximum grounding start dates. The uncertainty of the duration estimates is incorporated in the minimum and maximum start dates.

tinental shelf occurred at 11.5 ± 0.3 cal kyr BP (Bart et al., 2018). Bart and Cone (2012) proposed the GCB stillstand ended at 27.5 cal kyr BP. A pre-LGM retreat is precluded because data presented by Halberstadt et al. (2016) require that ice remained grounded in both the GCB and LAB until after a grounding line embayment opened in the WDB at 11.5 cal kyr BP (Bart and Kratochvil, 2022). The oldest date from deglacial sediment overlying the foreset of the middle continental shelf GZW in the GCB requires that the stillstand had ended by 8.7 cal kyr BP (Bart and Cone, 2012). We apply the same age of retreat (8.7 cal kyr) to the LAB middle continental shelf stillstand because the only other radiocarbon ages are from core tops.

Our data do not support previous studies that suggested that retreat occurred in a gradual lockstep fashion (Conway et al., 1999). Instead, both the chronology and stillstand duration data suggest that grounding line retreat proceeded in an unsteady episodic retreat style within individual troughs (Table 5 and Fig. 5). The earliest retreat in the DT may be partly related to the greater depth of the DT. The subsequent opening of an embayment in the PT may have been related to its small catchment area that delivered relatively low volumes of ice to the grounding zone. The sustained grounding in the JB may have been associated with both its larger catchment, flow capture from the PT catchment, and buttressing from its adjacent broad shallow banks. The long stillstand duration in the WDB may have been aided by antecedent topography that includes a bottleneck constriction at the location of the middle continental shelf grounding stillstand (Danielson and Bart, 2019) plus the apparent rapid sediment aggradation

following ice shelf break up at 12.3 cal kyr BP (Bart and Tulaczyk, 2020). The available age control (see above) suggests that up to 3 millennia may have elapsed before grounded ice retreated from the GCB and LAB, but here the chronologies are poorly constrained.

We acknowledge that the retreat chronology is likely to change as more radiocarbon data are generated. With the available constraints, our data support other previous studies that suggested that retreat was not synchronous or in lockstep between troughs (Halberstadt et al., 2016; Prothro et al., 2020; Mosola and Anderson, 2006). Neither the onset, duration, or termination of Ross Sea stillstands appear to be related to global or regional-scale forcing mechanisms with the possible exception of the WDB middle continental shelf stillstand which may be bracketed between intervals of rapid, large-amplitude sea-level rise at meltwater pulses (MWPs) 1a and 1b (Lin et al., 2021). These data are not consistent with the view that WAIS and EAIS contraction in the Ross Sea contributed significantly to the sustained sea-level rise during either MWP 1a or 1b. An asynchronous opening of grounding line embayments would have been associated with multiple episodes of short-lived accelerated sea-level rise. The marked sinuosity of the modern grounding line in the Ross Sea suggests that this staggered retreat persists through to the present.

5 Conclusion

Given the inherent uncertainties in our approach, we acknowledge that future work should focus on more directly constraining onset, duration, and cessation of grounding zone stillstands with radiocarbon data. With the available chronologic data, seismic mapping of GZWs provides reasonable first-order estimates for stillstand duration. The locations and sediment volumes of GZWs suggest millennial- to centennial-duration stillstands for Ross Sea ice streams during the early phases of the post-LGM retreat followed by a shift to significantly shorter stillstands. Combined with the available age control, our first-order duration estimates strongly suggest a staggered retreat that formed deep grounding line embayments between troughs. These results can be used as inputs to ice sheet models to better constrain contributions to the post-LGM sea-level rise as the deglacial period progressed in the Ross Sea. Asynchronous collapse of individual catchments occurring over the course of the post-LGM suggests that the Ross Sea sector contributed to multiple episodes of relatively small-amplitude sea-level rise rather than fewer intervals of rapid large-amplitude sea-level changes from a regionally synchronous retreat. The high sinuosity of the modern grounding zone in the Ross Sea suggests that this retreat style persists.

Appendix A: Catalogue of Ross Sea GZWs

The GZWs mapped in this study match those identified in other regional studies using seismic data and multibeam bathymetry (Table S3). In the LAB all three of the mapped GZWs (Fig. 4a–c; Table 1) have been previously identified from NBP9902 multibeam and seismic lines as GZWs 6c, 6b, and 6a in Mosola and Anderson (2006). In the WDB, the outer shelf GZW (Fig. 4d; Table 1) has been mapped using seismic surveys such as PD90, NBP9307, NBP9501, NBP9902, NBP0802, and NBP1502. It has previously been identified as GZW 5c in Mosola and Anderson (2006) using multibeam data. The WDB middle shelf GZW (Fig. 4e; Table 1) was previously identified as GZW 5b in Mosola and Anderson (2006) and as the composite GZW mapped using the NBP1502B multibeam survey (Bart et al., 2017). The outer shelf and middle shelf GZWs in the GCB (Fig. 4f and g; Table 1) were identified in the seismic surveys PD90, NBP9401, NBP9501, NBP0301A, and NBP0802 as the Brown Unit GZW and the Gray Unit GZW, respectively (Bart and Owolana, 2012). The GCB inner reaches east GZW (Fig. 4h; Table 1) was previously mapped from a regional multibeam bathymetry study as G4 (Halberstadt et al., 2016). The two inner reaches GZWs in the western GCB (Fig. 4i and j; Table 1) have been identified and mapped for this study. The middle shelf GZW in the PT (Fig. 4k; Table 1) was first identified using the seismic surveys of NBP9401 and NBP9501 (Shipp et al., 1999). Multibeam surveys and cores from NBP1502A further studied the middle shelf GZW in the PT (Prothro et al., 2020). The middle shelf GZWs in the JB and DT (Fig. 4l and o; Table 1) were first identified using the seismic surveys of NBP9401 and NBP9501 (Shipp et al., 1999). Additional cores were collected from the middle shelf GZW in the JB (Fig. 4l; Table 1) during NBP1502A (Prothro et al., 2020). The interior JB GZW near Franklin Island (Fig. 4m; Table 1) has been identified from legacy multibeam bathymetry and new multibeam bathymetry collected during NBP1502A and has been cored (Halberstadt et al., 2016; Prothro et al., 2020; Simkins et al., 2017; Greenwood et al., 2018). The DT inner reaches GZWs (Fig. 4p and q; Table 1) were previously mapped using the IT90RS seismic survey as well as multibeam data from PNRA 2006, NBP0801, NBP1704, and NBP1801 (Baroni et al., 2022).

Table A1. Catalogue of Ross Sea grounding zone wedges.

GZW location		References
a.	LAB outer shelf	GZW 6c (Mosola and Anderson, 2006)
b.	LAB middle shelf	GZW 6b (Mosola and Anderson, 2006)
c.	LAB middle shelf inner reaches	GZW 6a (Mosola and Anderson, 2006)
d.	WDB outer shelf	GZW 5c (Mosola and Anderson, 2006)
e.	WDB middle shelf	Composite GZW (Bart et al., 2017)
f.	GCB outer shelf	Brown Unit GZW (Bart and Owolana, 2012)
g.	GCB middle shelf west	Gray Unit GZW (Bart and Owolana, 2012)
h.	GCB inner reaches east	G4 (Halberstadt et al., 2016)
i.	GCB inner reaches west	This study
j.	GCB inner reaches Ross Bank	This study
k.	PT middle shelf	Shipp et al. (1999); Prothro et al. (2020)
l.	JOIDES middle shelf	Shipp et al. (1999); Prothro et al. (2020)
m.	JOIDES inner reaches 1	Simkins et al. (2017); Prothro et al. (2020); Greenwood et al. (2018)
n.	JOIDES inner reaches 2	This study
o.	DT outer shelf	Shipp et al. (1999)
p.	DT inner reaches 1	Baroni et al. (2022)
q.	DT inner reaches 2	Baroni et al. (2022)

Data availability. The data that support the findings of this study are openly available in the Antarctic Seismic Data Library System hosted at OGS at https://sdls.ogs.trieste.it/cache/index.jsp (OGS, 2022; Wardell et al., 2007). A full list of seismic surveys used in this study is given in Table S1.

Supplement. The supplement related to this article is available online at: https://doi.org/10.5194/tc-18-1125-2024-supplement.

Author contributions. MD performed the mapping of the seismic data and figure generation; MD and PB interpreted the results; MD and PB wrote and edited the paper.

Competing interests. The contact author has declared that neither of the authors has any competing interests.

Disclaimer. Publisher's note: Copernicus Publications remains neutral with regard to jurisdictional claims made in the text, published maps, institutional affiliations, or any other geographical representation in this paper. While Copernicus Publications makes every effort to include appropriate place names, the final responsibility lies with the authors.

Special issue statement. This article is part of the special issue "Icy landscapes of the past". It is not associated with a conference.

Acknowledgements. Support for the project was provided by a United States National Science Foundation Office of Polar Programs Antarctic Earth Sciences Division grant (no. 1841136) to Philip J. Bart. Seismic data used for this project were accessed from the Antarctic Seismic Data Library System (SDLS) hosted at the National Institute of Oceanography and Applied Geophysics (OGS). We thank the original collectors of these data. A full list of the seismic surveys used can be found in Table S1.

Financial support. This research has been supported by the Office of Polar Programs (grant no. 1841136).

Review statement. This paper was edited by Yusuke Suganuma and reviewed by Lindsay O. Prothro and Johann Philipp Klages.

References

Alley, R. B., Blankenship, D. D., Bentley, C. R., and Rooney, S. T.: Deformation of till beneath ice stream B, West Antarctica, Letters to Nature, 322, 57–59, 1986.

Alley, R. B., Blankenship, D. D., Bentley, C. R., and Rooney, S. T.: Till beneath ice stream B: 3. Till deformation: Evidence and implications, J. Geophys. Res., 92, 8921–8929, https://doi.org/10.1029/JB092iB09p08921, 1987.

Alley, R. B., Blankenship, D. D., Rooney, S. T., and Bentley, C. R.: Sedimentation beneath ice shelves – the view from ice stream B, Mar. Geol., 85, 101–120, 1989.

Alley, R. B., Anandakrishnan, S., Dupont, T. K., Parizek, B. R., and Pollard, D.: Effect of Sedimentation on Ice-Sheet Grounding-Line Stability, Sci. Rep.-UK, 315, 1838–1840, 2007.

Anandakrishnan, S., Catania, G. A., Alley, R. B., and Horgan, H. J.: Discovery of Till Deposition at the Grounding Line of Whillans Ice Stream, Sci. Rep.-UK, 315, 1835–1837, 2007.

Anderson, J. B. and Bartek, L. R.: Cenozoic Glacial History of the Ross Sea Revealed by Intermediate Resolution Seismic Reflection Data Combined with Drill Site Information, in: The Antarctic Paleoenvironment: A Perspective on Global Change: Part One, Antarctic Research Series, 231–264, https://doi.org/10.1029/AR056p0231, 1992.

Anderson, J. B., Conway, H., Bart, P. J., Witus, A. E., Greenwood, S. L., McKay, R. M., Hall, B. L., Ackert, R. P., Licht, K., Jakobsson, M., and Stone, J. O.: Ross Sea paleo-ice sheet drainage and deglacial history during and since the LGM, Quaternary Sci. Rev., 100, 31–54, https://doi.org/10.1016/j.quascirev.2013.08.020, 2014.

Baroni, C., Tenti, M., Bart, P., Salvatore, M. C., Gasperini, L., Busetti, M., Sauli, C., Stucchi, E. M., and Tognarelli, A.: Antarctic Ice Sheet re-advance during the Antarctic Cold Reversal identified in the Western Ross Sea, Geogr. Fis.Din. Quat., 45, 3–18, 2022.

Bart, P. and De Santis, L.: Glacial Intensification During the Neogene: A Review of Seismic Stratigraphic Evidence from the Ross Sea, Antarctica, Continental Shelf, Oceanography, 25, 166–183, https://doi.org/10.5670/oceanog.2012.92, 2012.

Bart, P. J. and Cone, A. N.: Early stall of West Antarctic Ice Sheet advance on the eastern Ross Sea middle shelf followed by retreat at 27,500 ^{14}C yr BP, Palaeogeogr. Palaeocl., 335–336, 52–60, https://doi.org/10.1016/j.palaeo.2011.08.007, 2012.

Bart, P. J. and Kratochvil, M.: A paleo-perspective on West Antarctic Ice Sheet retreat, Sci. Rep.-UK, 12, 17693, https://doi.org/10.1038/s41598-022-22450-3, 2022.

Bart, P. J. and Owolana, B.: On the duration of West Antarctic Ice Sheet grounding events in Ross Sea during the Quaternary, Quaternary Sci. Rev., 47, 101–115, https://doi.org/10.1016/j.quascirev.2012.04.023, 2012.

Bart, P. J. and Tulaczyk, S.: A significant acceleration of ice volume discharge preceded a major retreat of a West Antarctic paleo-ice stream, Geology, 48, 313–317, https://doi.org/10.1130/g46916.1, 2020.

Bart, P. J., Krogmeier, B. J., Bart, M. P., and Tulaczyk, S.: The paradox of a long grounding during West Antarctic Ice Sheet retreat in Ross Sea, Sci. Rep.-UK, 7, 1262, https://doi.org/10.1038/s41598-017-01329-8, 2017.

Bart, P. J., DeCesare, M., Rosenheim, B. E., Majewski, W., and McGlannan, A.: A centuries-long delay between a paleo-ice-shelf collapse and grounding-line retreat in the Whales Deep Basin, eastern Ross Sea, Antarctica, Sci. Rep.-UK, 8, 12392, https://doi.org/10.1038/s41598-018-29911-8, 2018.

Batchelor, C. L. and Dowdeswell, J. A.: Ice-sheet grounding-zone wedges (GZWs) on high-latitude continental margins, Mar. Geol., 363, 65–92, https://doi.org/10.1016/j.margeo.2015.02.001, 2015.

Christoffersen, P., Tulaczyk, S., and Behar, A.: Basal ice sequences in Antarctic ice stream: Exposure of past hydrologic conditions and a principal mode of sediment transfer, J. Geophys. Res., 115, 1–12, https://doi.org/10.1029/2009jf001430, 2010.

Cochrane, G. R., Cooper, A. K., Childs, J. R., and Hart, P. E.: USGS seismic refraction surveys in the Ross Sea, 1984–1990, USGS Openfile Reports, 92–556, 1992.

Cochrane, G. R., De Santis, L., and Cooper, A. K.: Seismic velocity expression of glacial sedimentary rocks beneath the Ross Sea from sonobuoy seismic-refraction data, in: Geology and Seismic Stratigraphy of the Antarctic Margin, Antarctic Research Series, 68, 261–270, 1995.

Conway, H., Hall, B. L., Denton, G. H., Gades, A. M., and Waddington, E. D.: Past and Future Grounding-Line Retreat of the West Antarctic Ice Sheet, Science, 286, 280–283, https://doi.org/10.1126/science.286.5438.280, 1999.

Cuffey, K. M., Clow, G. D., Steig, E. J., Buizert, C., Fudge, T. J., Koutnik, M., Waddington, E. D., Alley, R. B., and Severinghaus, J. P.: Deglacial temperature history of West Antarctica, P. Natl. Acad. Sci. USA, 113, 14249–14254, https://doi.org/10.1073/pnas.1609132113, 2016.

Cunningham, W. L., Leventer, A., Andrews, J. T., Jennings, A. E., and Licht, K. J.: Late Pleistocene-Holocene marine conditions in the Ross Sea, Antarctica: evidence from the diatom record, Holocene, 9, 129–139, https://doi.org/10.1191/095968399675624796, 1999.

Danielson, M. and Bart, P. J.: Topographic control on the post-LGM grounding zone locations of the West Antarctic Ice Sheet in the Whales Deep Basin, Eastern Ross Sea, Mar. Geol., 407, 248–260, https://doi.org/10.1016/j.margeo.2018.11.001, 2019.

Davey, F. J. and Nitsche, F.: Ross Sea bathymetry grid (2005) based on Fred Davey's bathymetry map (2004), IEDA, https://doi.org/10.1594/IEDA/100405, 2013.

Domack, E. W., Jacobson, E. A., Shipp, S., and Anderson, J. B.: Late Pleistocene–Holocene retreat of the West Antarctic Ice-Sheet system in the Ross Sea: Part 2–Sedimentologic and stratigraphic signature, Geol. Soc. Am. Bull., 111, 1517–1536, 1999.

Dorschel, B., Hehemann, L., Viquerat, S., Warnke, F., Dreutter, S., Tenberge, Y. S., Accettella, D., An, L., Barrios, F., Bazhenova, E., Black, J., Bohoyo, F., Davey, C., De Santis, L., Dotti, C. E., Fremand, A. C., Fretwell, P. T., Gales, J. A., Gao, J., Gasperini, L., Greenbaum, J. S., Jencks, J. H., Hogan, K., Hong, J. K., Jakobsson, M., Jensen, L., Kool, J., Larin, S., Larter, R. D., Leitchenkov, G., Loubrieu, B., Mackay, K., Mayer, L., Millan, R., Morlighem, M., Navidad, F., Nitsche, F. O., Nogi, Y., Pertuisot, C., Post, A. L., Pritchard, H. D., Purser, A., Rebesco, M., Rignot, E., Roberts, J. L., Rovere, M., Ryzhov, I., Sauli, C., Schmitt, T., Silvano, A., Smith, J., Snaith, H., Tate, A. J., Tinto, K., Vandenbossche, P., Weatherall, P., Wintersteller, P., Yang, C., Zhang, T., and Arndt, J. E.: The International Bathymetric Chart of the Southern Ocean Version 2, Sci. Data, 9, 275, https://doi.org/10.1038/s41597-022-01366-7, 2022.

Dowdeswell, J. A. and Fugelli, E. M. G.: The seismic architecture and geometry of grounding-zone wedges formed at the marine margins of past ice sheets, Geol. Soc. Am. Bull., 124, 1750–1761, https://doi.org/10.1130/b30628.1, 2012.

Dowdeswell, J. A., Hogan, K. A., and Le Heron, D. P.: The glacier-influenced marine record on high-latitude continental margins: synergies between modern, Quaternary and ancient evidence, Geological Society, London, Special Publications, 475, 261–279, https://doi.org/10.1144/sp475.13, 2019.

Elverhøi, A., Hooke, R. L., and Solheim, A.: Late cenozoic erosion and sediment yield from the Svalbardðbarents Sea region: Impli-

cations for understanding erosion of glacierized basins, Quaternary Sci. Rev., 17, 209–241, 1998.

Greenwood, S. L., Simkins, L. M., Winsborrow, M. C. M., and Bjarnadóttir, L. R.: Exceptions to bed-controlled ice sheet flow and retreat from glaciated continental margins worldwide, Science Advances, 7, 1–12, 2021.

Greenwood, S. L., Simkins, L. M., Halberstadt, A. R. W., Prothro, L. O., and Anderson, J. B.: Holocene reconfiguration and readvance of the East Antarctic Ice Sheet, Nat. Commun., 9, 3176, https://doi.org/10.1038/s41467-018-05625-3, 2018.

Halberstadt, A. R. W., Simkins, L. M., Greenwood, S. L., and Anderson, J. B.: Past ice-sheet behaviour: retreat scenarios and changing controls in the Ross Sea, Antarctica, The Cryosphere, 10, 1003–1020, https://doi.org/10.5194/tc-10-1003-2016, 2016.

Hallet, B., Hunter, L., and Bogen, J.: Rates of erosion and sediment evacuation by glaciers: A review of field data and their implications, Global Planet. Change, 12, 213–235, 1996.

Jordan, T. A., Riley, T. R., and Siddoway, C. S.: The geological history and evolution of West Antarctica, Nature Reviews Earth & Environment, 1, 117–133, https://doi.org/10.1038/s43017-019-0013-6, 2020.

Joughin, I. and Alley, R. B.: Stability of the West Antarctic ice sheet in a warming world, Nat. Geosci., 4, 506–513, https://doi.org/10.1038/ngeo1194, 2011.

Kingslake, J., Scherer, R. P., Albrecht, T., Coenen, J., Powell, R. D., Reese, R., Stansell, N. D., Tulaczyk, S., Wearing, M. G., and Whitehouse, P. L.: Extensive retreat and re-advance of the West Antarctic Ice Sheet during the Holocene, Nature, 558, 430–434, https://doi.org/10.1038/s41586-018-0208-x, 2018.

Klages, J. P., Kuhn, G., Hillenbrand, C. D., Graham, A. G. C., Smith, J. A., Larter, R. D., Gohl, K., and Wacker, L.: Retreat of the West Antarctic Ice Sheet from the western Amundsen Sea shelf at a pre- or early LGM stage, Quaternary Sci. Rev., 91, 1–15, https://doi.org/10.1016/j.quascirev.2014.02.017, 2014.

Klages, J. P., Kuhn, G., Graham, A. G. C., Hillenbrand, C. D., Smith, J. A., Nitsche, F. O., Larter, R. D., and Gohl, K.: Palaeo-ice stream pathways and retreat style in the easternmost Amundsen Sea Embayment, West Antarctica, revealed by combined multibeam bathymetric and seismic data, Geomorphology, 245, 207–222, https://doi.org/10.1016/j.geomorph.2015.05.020, 2015.

Koppes, M. N. and Montgomery, D. R.: The relative efficacy of fluvial and glacial erosion over modern to orogenic timescales, Nat. Geosci., 2, 644–647, https://doi.org/10.1038/ngeo616, 2009.

Li, X., Zattin, M., and Olivetti, V.: Apatite Fission Track Signatures of the Ross Sea Ice Flows During the Last Glacial Maximum, Geochem. Geophy. Geosy., 21, 1–22, https://doi.org/10.1029/2019gc008749, 2020.

Licht, K. J. and Palmer, E. F.: Erosion and transport by Byrd Glacier, Antarctica during the Last Glacial Maximum, Quaternary Sci. Rev., 62, 32–48, https://doi.org/10.1016/j.quascirev.2012.11.017, 2013.

Licht, K. J., Lederer, J. R., and Jeffrey Swope, R.:

Licht, K. J., Hennessy, A. J., and Welke, B. M.: The U-Pb detrital zircon signature of West Antarctic ice stream tills in the Ross embayment, with implications for Last Glacial Maximum ice flow reconstructions, Antarct. Sci., 26, 687–697, https://doi.org/10.1017/s0954102014000315, 2014. Provenance of LGM glacial till (sand fraction) across the Ross embayment, Antarctica, Quaternary Sci. Rev., 24, 1499–1520, https://doi.org/10.1016/j.quascirev.2004.10.017, 2005.

Lin, Y., Hibbert, F. D., Whitehouse, P. L., Woodroffe, S. A., Purcell, A., Shennan, I., and Bradley, S. L.: A reconciled solution of Meltwater Pulse 1A sources using sea-level fingerprinting, Nat. Commun., 12, 2015, https://doi.org/10.1038/s41467-021-21990-y, 2021.

Livingstone, S. J., Stokes, C. R., Ó Cofaigh, C., Hillenbrand, C.-D., Vieli, A., Jamieson, S. S. R., Spagnolo, M., and Dowdeswell, J. A.: Subglacial processes on an Antarctic ice stream bed. 1: Sediment transport and bedform genesis inferred from marine geophysical data, J. Glaciol., 62, 270–284, https://doi.org/10.1017/jog.2016.18, 2016.

Lowry, D. P., Golledge, N. R., Bertler, N. A. N., Jones, R. S., McKay, R., and Stutz, J.: Geologic controls on ice sheet sensitivity to deglacial climate forcing in the Ross Embayment, Antarctica, Quaternary Science Advances, 1, 1–17, https://doi.org/10.1016/j.qsa.2020.100002, 2020.

McKenzie, M. A., Miller, L. E., Slawson, J. S., MacKie, E. J., and Wang, S.: Differential impact of isolated topographic bumps on ice sheet flow and subglacial processes, The Cryosphere, 17, 2477–2486, https://doi.org/10.5194/tc-17-2477-2023, 2023.

Mosola, A. B. and Anderson, J. B.: Expansion and rapid retreat of the West Antarctic Ice Sheet in eastern Ross Sea: possible consequence of over-extended ice streams?, Quaternary Sci. Rev., 25, 2177–2196, https://doi.org/10.1016/j.quascirev.2005.12.013, 2006.

Mouginot, J., Scheuchl, B., and Rignot, E.: MEaSUREs Antarctic Boundaries for IPY 2007–2009 from Satellite Radar, Version 2, NASA National Snow and Ice Data Center [data set], https://doi.org/10.5067/AXE4121732AD, 2017.

OGS: Antarctic Seismic Data Library System (SDLS), https://sdls.ogs.trieste.it/cache/index.jsp, last access: January 2022.

Pérez, L. F., De Santis, L., McKay, R. M., Larter, R. D., Ash, J., Bart, P. J., Böhm, G., Brancatelli, G., Browne, I., Colleoni, F., Dodd, J. P., Geletti, R., Harwood, D. M., Kuhn, G., Sverre Laberg, J., Leckie, R. M., Levy, R. H., Marschalek, J., Mateo, Z., Naish, T. R., Sangiorgi, F., Shevenell, A. E., Sorlien, C. C., van de Flierdt, T., and International Ocean Discovery Program Expedition Scientists: Early and middle Miocene ice sheet dynamics in the Ross Sea: Results from integrated core-log-seismic interpretation, GSA Bull., 134, 348–370, https://doi.org/10.1130/B35814.1, 2021.

Powell, R. D., Dawber, M., McInnes, J. N., and Pyne, A. R.: Observations of the grounding-line area at a floating glacier terminus, Ann. Glaciol., 22, 217–223, https://doi.org/10.3189/1996AoG22-1-217-223, 1996.

Prothro, L. O., Simkins, L. M., Majewski, W., and Anderson, J. B.: Glacial retreat patterns and processes determined from integrated sedimentology and geomorphology records, Mar. Geol., 395, 104–119, https://doi.org/10.1016/j.margeo.2017.09.012, 2018.

Prothro, L. O., Majewski, W., Yokoyama, Y., Simkins, L. M., Anderson, J. B., Yamane, M., Miyairi, Y., and Ohkouchi, N.: Timing and pathways of East Antarctic Ice Sheet retreat, Quaternary Sci. Rev., 230, 1–20, https://doi.org/10.1016/j.quascirev.2020.106166, 2020.

Rignot, E., Jacobs, S., Mouginot, J., and Scheuchl, B.: Ice-Shelf Melting Around Antarctica, Sci. Rep.-UK, 341, 266–270, 2013.

Schlunegger, F., Melzer, J., and Tucker, G.: Climate, exposed source-rock lithologies, crustal uplift and surface erosion: a theoretical analysis calibrated with data from the Alps/North Alpine Foreland Basin system, Int. J. Earth Sci., 90, 484–499, https://doi.org/10.1007/s005310100174, 2001.

Shipp, S., Anderson, J., and Domack, E.: Late Pleistocene–Holocene retreat of the West Antarctic Ice-Sheet system in the Ross Sea: Part 1–Geophysical results, Geol. Soc. Am. Bull., 111, 1486–1519, https://doi.org/10.1130/0016-7606(1999)111<1486:Lphrot>2.3.Co;2, 1999.

Simkins, L. M., Anderson, J. B., Greenwood, S. L., Gonnermann, H. M., Prothro, L. O., Halberstadt, A. R. W., Stearns, L. A., Pollard, D., and DeConto, R. M.: Anatomy of a meltwater drainage system beneath the ancestral East Antarctic ice sheet, Nat. Geosci., 10, 691–697, https://doi.org/10.1038/ngeo3012, 2017.

Tinto, K. J., Padman, L., Siddoway, C. S., Springer, S. R., Fricker, H. A., Das, I., Caratori Tontini, F., Porter, D. F., Frearson, N. P., Howard, S. L., Siegfried, M. R., Mosbeux, C., Becker, M. K., Bertinato, C., Boghosian, A., Brady, N., Burton, B. L., Chu, W., Cordero, S. I., Dhakal, T., Dong, L., Gustafson, C. D., Keeshin, S., Locke, C., Lockett, A., O'Brien, G., Spergel, J. J., Starke, S. E., Tankersley, M., Wearing, M. G., and Bell, R. E.: Ross Ice Shelf response to climate driven by the tectonic imprint on seafloor bathymetry, Nat. Geosci., 12, 441–449, https://doi.org/10.1038/s41561-019-0370-2, 2019.

Wardell, N., Childs, J. R., and Cooper, A. K.: Advances through collaboration: sharing seismic reflection data via the Antarctic Seismic Data Library System for Cooperative Research (SDLS), Antarctica: a keystone in a changing world-online proceedings of the 10th ISAES, https://doi.org/10.3133/of2007-1047.srp001, 2007.

Weertman, J.: Stability of the Junction of an Ice Sheet and an Ice Shelf, J. Glaciol., 13, 3–11, https://doi.org/10.3189/s0022143000023327, 1974.

Wilson, D. S. and Luyendyk, B. P.: Bedrock platforms within the Ross Embayment, West Antarctica: Hypotheses for ice sheet history, wave erosion, Cenozoic extension, and thermal subsidence, Geochem. Geophy. Geosy., 7, 1–23, https://doi.org/10.1029/2006gc001294, 2006.